

## Thin Film of Copper Hexacyanoferrate Dispersed on the Surface of a Conducting Carbon Ceramic Material, SiO<sub>2</sub>/ZrO<sub>2</sub>/C-Graphite: Characteristics and Electrochemical Studies

Eduardo Marafon,<sup>a</sup> Alzira M.S. Lucho,<sup>a</sup> Maria S.P. Francisco,<sup>a</sup> Richard Landers<sup>b,c</sup>  
and Yoshitaka Gushikem<sup>\*,a</sup>

<sup>a</sup>Instituto de Química, Universidade Estadual de Campinas, CP 6154, 13084-862 Campinas-SP, Brazil

<sup>b</sup>Instituto de Física Gleb Wataghin, Universidade Estadual de Campinas, CP 6165, 13083-970 Campinas SP, Brazil

<sup>c</sup>Laboratório Nacional de Luz Síncrotron (LNLS), CP 6192, 13083-970 Campinas SP, Brazil

O material SiO<sub>2</sub>/ZrO<sub>2</sub>/C-graphite (SZC) foi preparado pelo método sol-gel apresentando duas composições, designadas por: (a) SZC30 (SiO<sub>2</sub>= 50%, ZrO<sub>2</sub>= 20%, C= 30%) e (b) SZC20 (SiO<sub>2</sub>=60%, ZrO<sub>2</sub>= 20%, C= 20%) em % m. A estrutura do material foi investigada por difração de raios X (XRD), microscopia eletrônica de transmissão de alta resolução (HR-TEM) e espectroscopia de fotoelétrons excitados por raios X (XPS). A condutividade elétrica dos discos prensados destes materiais foi 4 e 18 S cm<sup>-1</sup> para SZC20 e SZC30, e a área superficial específica (determinado pelo método BET) dos compósitos carbono cerâmico foi 45 e 12 m<sup>2</sup> g<sup>-1</sup>, respectivamente. Um filme fino de hexacianoferrato(II) de cobre foi formado *in situ* na superfície do material contendo 30 % (em massa) de grafite (SZC30). A espessura do filme foi estimada como sendo 110 nm. O potencial médio para o processo redox foi dependente da concentração de eletrólito suporte na faixa de 0,1 a 1,0 mol L<sup>-1</sup> de KCl e a resistência de transferência de carga, determinada por espectroscopia de impedância eletroquímica (EIS), foi de 23,8 ohm cm<sup>2</sup>.

SiO<sub>2</sub>/ZrO<sub>2</sub>/C-graphite materials (SZC) were prepared by the sol-gel method presenting two compositions and designated as: (a) SZC30 (SiO<sub>2</sub>= 50%, ZrO<sub>2</sub>= 20%, C= 30%) and (b) SZC20 (SiO<sub>2</sub>=60%, ZrO<sub>2</sub>= 20%, C= 20%) in wt.%. The material structure was investigated by X-ray diffraction (XRD), high resolution transmission electron microscopy (HR-TEM) and X-ray photoelectron spectroscopy (XPS). The electrical conductivities obtained for the pressed disks of these materials were 4 and 18 S cm<sup>-1</sup> for SZC20 and SZC30, and the specific surface areas (determined by the BET method) of the carbon ceramic composites were 45 and 12 m<sup>2</sup> g<sup>-1</sup>, respectively. A copper hexacyanoferrate thin film was grown *in situ* on the material surface containing 30 wt.% C (SZC30). The thickness of the film was estimated as 110 nm. The midpoint potential for the redox process was dependent on the KCl supporting electrolyte concentrations in the range between 0.1 and 1.0 mol L<sup>-1</sup> and the charge transfer resistance determined by electrochemical impedance spectroscopy experiment was 23.8 ohm cm<sup>2</sup>.

**Keywords:** silica-zirconia-graphite, carbon ceramic material, conducting ceramic material, copper hexacyanoferrate film

### Introduction

Transition metal hexacyanoferrates have been the subject of widespread interest because of their electrocatalytic, electrochromic, ion exchange, ion sensing and photomagnetic properties, as recently pointed out in a review where electrosynthesis, *in situ* characterization and technological applications of Prussian Blue analogues are

emphasized.<sup>1</sup> These metal hexacyanoferrate compounds are usually prepared by chemical and electrochemical methods. To support films of these materials on solid surfaces, when necessary, inert substrates such as glassy carbon, graphite, platinum or gold have been used.<sup>2-7</sup> Porous substrates such as SiO<sub>2</sub> coated with thin films of SnO<sub>2</sub>, TiO<sub>2</sub> and ZrO<sub>2</sub> have also been used as substrates to adhere several metal hexacyanoferrates.<sup>8-11</sup> These porous substrates allowed obtaining chemically stable and well adhered films of the metal hexacyanoferrates, presumably confined in the pores of these matrices. A disadvantage in

\*e-mail: gushikem@iqm.unicamp.br

using such substrates has been their high electrical resistance which can limit their widespread use.

New generations of materials presenting high electrical conductivity, designated as carbon ceramic materials, have been prepared by the sol-gel processing method<sup>12-14</sup> and their use as substrate materials to support electroactive species has been a subject of great interest in recent years.<sup>15-22</sup>

In this work, the experimental procedure for the preparation and characterization of the carbon ceramic material  $\text{SiO}_2/\text{ZrO}_2/\text{C}$  (SZC), where C refers to graphite particles confined inside the mixed oxide particles, are reported. The experimental technique of preparation was the sol-gel processing method as it allows obtaining solids possessing homogeneous distributions of the particles in the matrices.<sup>23-25</sup> Furthermore, a thin film of copper hexacyanoferrate (CuHCF) was prepared by an *in situ* reaction, on the SZC material surface. The electrochemical response of the copper hexacyanoferrate film and its thickness on the substrate surface were investigated by the cyclic voltammetry technique. In order to determine the value of the charge transfer resistance ( $R_{\text{CT}}$ ) and to simulate an equivalent circuit for the system, the electrochemical impedance spectroscopy (EIS) technique was used.

## Experimental

### *Preparation of $\text{SiO}_2/\text{ZrO}_2/\text{C}$ -graphite*

SZC carbon ceramic composite materials, with two different compositions were prepared by the sol-gel method according to a previously described procedure.<sup>26</sup> To a solution of TEOS (tetraethyl orthosilicate; Aldrich) in pure ethanol in a ratio 1:1 (v/v), an aqueous acid solution was added and the mixture, stirred for a few hours at room temperature. To the pre-hydrolysed TEOS solution, appropriate amount of zirconium tetrabutoxide (Aldrich) and C-graphite (Fluka,  $S_{\text{BET}} = 8 \text{ m}^2 \text{ g}^{-1}$ ) were added, followed by an additional small amount of the aqueous acid solution. The mixture was stirred and allowed to rest. The solvent was evaporated until gelation and the xerogel obtained was ground to a fine powder, washed exhaustively with bidistilled water and ethanol and, finally, dried under vacuum.

### *Specific surface area*

The specific surface areas,  $S_{\text{BET}}$ , were measured by the BET multipoint technique on a Micromeritics Flowsorb II 2300 apparatus connected to a flow controller.

### *X-ray diffraction*

The X-ray diffraction patterns were obtained by using a Shimadzu XRD 6000 apparatus. The following conditions were used: Cu  $K\alpha$  radiation ( $\lambda = 1.5405 \text{ \AA}$ ) at 40 kV, 30 mA current and a scan rate of  $2^\circ \text{ min}^{-1}$  in a range between  $5^\circ$  and  $50^\circ$  (in  $2\theta$ ).

### *High Resolution Transmission Electron Microscopy*

The high resolution transmission electron microscopy, HR-TEM, experiments were carried out at 300 kV on a JEOL JEM-3010 microscope at the Electronic Microscopy Laboratory of the National Synchrotron Light Laboratory, Campinas, Brazil, with a point resolution of 0.17 nm. The SZC fine powder was ultrasonically suspended in isopropyl alcohol for 10 minutes and the suspension deposited on a copper grid previously covered with a thin layer of carbon ( $\sim 30 \text{ \AA}$ ).

### *Scanning Electron Microscopy*

Scanning electron microscopy (SEM) was carried out using low vacuum microscopy (JSM 5900LV) at the Electronic Microscopy Laboratory of the National Synchrotron Light Laboratory in Campinas, Brazil, operating at an accelerating voltage of 25 kV. The samples were fixed onto double faced conducting tape adhered to an aluminum support and the images were obtained by using the secondary electrons.

### *Electrical conductivity*

To measure the electrical conductivity, a pressed circular disks with dimensions 13 mm diameter and 0.3 mm thickness were prepared for pure graphite, SZC20 and SZC30. The DC electrical conductivities were obtained by using the four-point probe according to the procedure of ASTM,<sup>27</sup> on an equipment using the source Keithley 617 and applying a potential between 0.005 and 0.050 V.

### *Film of copper hexacyanoferrate on $\text{SiO}_2/\text{ZrO}_2/\text{C}$ -graphite*

A disk of SZC with 8 mm diameter and approximately 2 mm thickness was obtained by pressing 40 mg of the finely divided powder of the material under  $5 \times 10^3 \text{ kg cm}^{-2}$  pressure. The disk obtained was immersed in 20 mL of  $2 \times 10^{-3} \text{ mol L}^{-1}$  copper acetate solution and allowed to rest for approximately 1 h and then washed with water in order to remove the physically adsorbed metal acetate.

The adsorption of  $\text{Cu}^{2+}$  ion on the matrix surface may occur mainly on the Brönsted acid sites  $\text{Zr-OH}^{28,29}$  according to the reaction described formally as:



In contact with an acidified solution of  $\text{K}_4[\text{Fe(CN)}_6]$ , a film of copper hexacyanoferrate complex of composition  $\text{K}_{4-2n}\text{Cu}_n[\text{Fe(CN)}_6]$  is formed on the surface.<sup>4</sup>

### X-ray photoelectron spectra

X-ray photoelectron spectroscopy of the disks modified with copper hexacyanoferrate and a disk of unmodified SZC were obtained with an HA100 VSW hemispherical analyzer operated in the fixed transmission mode (pass energy 44 eV), which gives a FWHM line width of 1.8 eV for the Au 4f 7/2 line. Al  $\text{K}\alpha$  radiation (1486.6 eV) was used for excitation. The pressure during the measurements was always less than  $2 \times 10^{-8}$  torr. Charging effects were corrected by shifting the spectra linearly so that the C1s line had a binding energy of 284.6 eV.<sup>30</sup>

### Electrochemical measurements

To carry out the electrochemical experiments, an electrode consisting of the disk glued at one end of a glass tube of 8 mm diameter and about 15 cm length was prepared. The electrical contact was made by a copper wire inserted inside the glass tube. To improve the connection between the metal and the disk surface, pure graphite powder was added.

The Autolab PGSTAT 20 potentiostat-galvanostat apparatus in conjunction with a three electrode system was used for the voltammetric measurements. A saturated calomel (SCE) reference electrode, a platinum wire counter electrode and the carbon ceramic electrode as the working electrode were employed for the electrochemical studies.

The impedance experiments were carried out on an Autolab/EchoChimie PGStat 30 apparatus. The experiments were made in a frequency range between 100 kHz and 10 MHz, applying 10 mV amplitude of sinusoidal voltage. The equivalent circuit was fitted using the FRA program.

## Results and Discussion

### Characterization of the materials

Chemical compositions of the materials obtained, the values of specific surface areas and the electrical

conductivities are presented in Table 1. Insertion of crystalline graphite into de ceramic material decreases the specific surface areas, *i.e.* 45 and 12  $\text{m}^2 \text{g}^{-1}$  for samples containing 20 and 30 wt.% of graphite, respectively, and the electrical conductivities are increased from 4 to 18  $\text{S cm}^{-1}$ .

**Table 1.** Summary of chemical compositions, specific surface areas,  $S_{\text{BET}}$ , and electrical conductivity

Samples	$\text{SiO}_2 /$ (wt.%)	$\text{ZrO}_2 /$ (wt.%)	Graphite / (wt.%)	$S_{\text{BET}} /$ ( $\text{m}^2 \text{g}^{-1}$ )	Conductivity / ( $\text{S cm}^{-1}$ )
SZC20	60	20	20	45	4
SZC30	50	20	30	12	18

The X-ray diffraction pattern for SZC30 (Figure not shown), as obtained, shows a strong peak at  $26.7^\circ$  (in  $2\theta$ ) corresponding to the interplanar distance of 0.34 nm (plane 002) and a weak one at  $44.6^\circ$  (in  $2\theta$ ) corresponding to the interplanar distance of 0.22 nm (plane 101) of crystalline graphite particle.<sup>31</sup> No diffraction peak due to  $\text{SiO}_2$  or  $\text{ZrO}_2$  is observed indicating that they are obtained as amorphous phases. Measurement carried for SZC20 sample gave similar results.

Figure 1 shows the HR-TEM micrograph for SZC20 as the representative image. The fringes appearing in the micrographs are due to the graphite particles since the ceramic part of the material, as obtained, is constituted of amorphous particles of  $\text{SiO}_2$  and  $\text{ZrO}_2$ . The fringes observed correspond to the crystallographic planes of graphite with interplanar distances of 0.34 and 0.26 nm, in accordance with the results obtained by XRD technique. The image shows graphite nanoparticles with dimensions of about 2.5 nm (selected encircled particles in the image) in the ceramic matrix. It is observed that

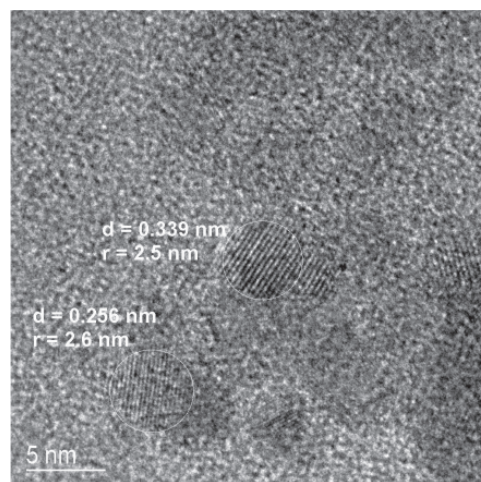


**Figure 1.** HR-TEM micrographs of confined nanospheres of carbon crystallites with radii around 2.5 nm in the SZC20 system.

these graphite particles are confined in the silica-zirconia matrix and it is also apparent that they present high degree of interconnection between them which can explain the good electrical conductivity of the materials obtained.

#### Copper hexacyanoferrate film on SZC surface

The nature of the intervalence complex formed *in situ* on the matrix surface, as probed by XPS is comparable to films produced by electrochemical or chemical procedures on substrate surfaces such as glassy carbon<sup>7</sup> carbon film<sup>32</sup> and porous mixed oxide surfaces.<sup>33</sup> The morphology of the surface of the SZC30 disk before and after deposition of the CuHCF film was monitored by analyses of SEM images.

Within the magnification used it is clear that comparing the roughness of the surface of the (SZC30) material (Figure 2A) increases after the CuHCF film deposition (Figure 2B).

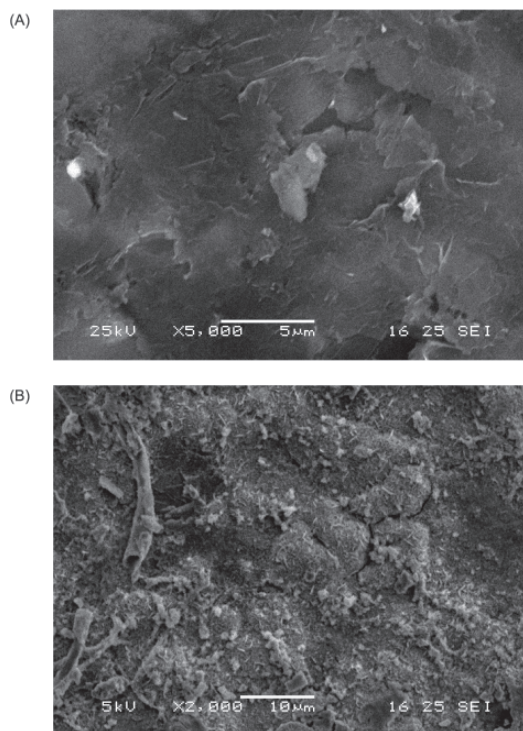


**Figure 2.** SEM images of SZC30 pressed disk (A) and coated with thin film CuHCF pressed disk (B).

**Table 2.** Binding energies (eV) for SZC/CuHCF and atoms concentrations

Sample	Binding Energy / (eV)			Concentration / (atom %)		
	Fe 2p <sub>3/2</sub>	Cu 2p <sub>3/2</sub>	N 1s	Fe	Cu	N
SZC20/CuHCF	707.6	931.8	397.0	1.3	0.8	7.8
SZC30/CuHCF	707.9	932.0	397.3	1.6	0.9	11.5

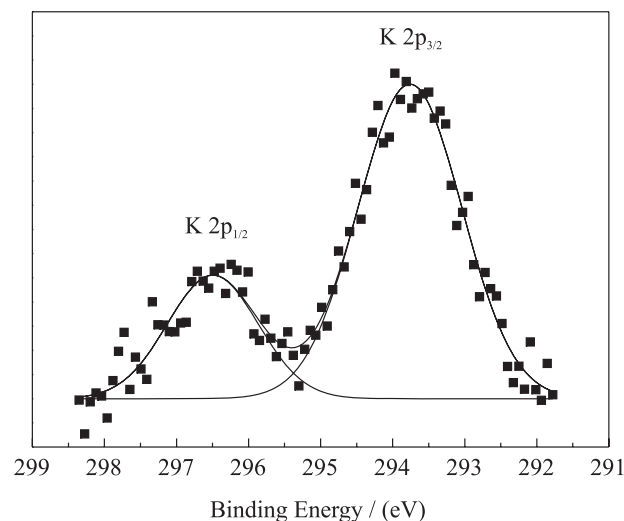
Chemical analyses of the disk surface for Fe, Cu and N and the respective binding energies data determined by XPS are presented in Table 2. The Cu/Fe atomic ratios determined were 0.6 for both samples and the N/Fe atomic ratios was 6 for SZC20/CuHCF and 7 for SZC30/CuHCF. The values obtained are reasonable considering the error associated in the present case (between 10-20 %).

Potassium ions could also be detected on the surface as show by the peaks observed at 292 eV (Figure 3) assigned to K2p<sub>3/2</sub> BE and at 296 eV assigned to K2p<sub>1/2</sub> BE.<sup>34</sup> These ions are incorporated into the copper hexacyanoferrate structure during the film formation process on the substrate surface and not physically adsorbed. Potassium ions are always detected, even after exhaustive washing of the disk with bidistilled water. A rough estimation of the atom percent on the surface gives the following values: a) SZC20: K = 0.6 atom % and b) SZC30: K = 0.7 atom %.

Other peaks of interest and not presented in Table 2 are the Zr 3d<sub>5/2</sub> BE peak observed for SZC30/CuHCF and SZC20/CuHCF at 182.1 and 182.2 eV, respectively. For pure ZrO<sub>2</sub>, this peak is observed at 182.2 eV.<sup>35</sup>

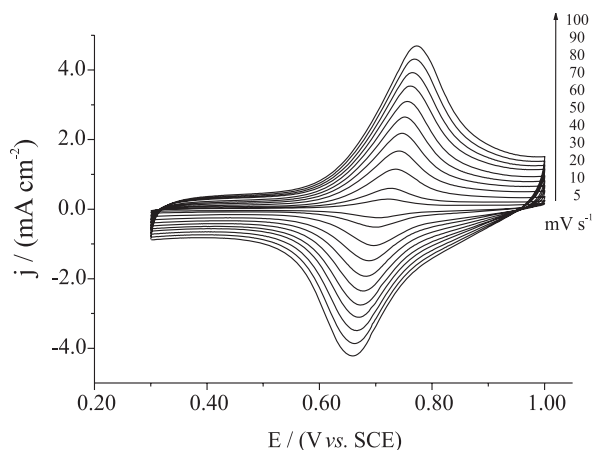
#### Electrochemical studies

Figure 4 shows the cyclic voltammetry curves for SZ30/CuHCF in the potential sweeping range between 0.3



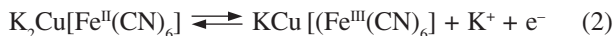
**Figure 3.** Binding energy peaks K2p<sub>1/2</sub> and K2p<sub>3/2</sub> of K<sup>+</sup> incorporated into the SZC20/CuHCF film.

and 1.0 V and sweeping rates between 5 and 100 mV s<sup>-1</sup>. A well-defined redox pair with mid-point potential,  $E_m = 0.69$  V ( $E_m = (E_{pa} + E_{pc})/2$ , where  $E_{pa}$  and  $E_{pc}$  are the anodic and cathodic peak potentials, respectively), is observed in 1.0 mol L<sup>-1</sup> KCl supporting electrolyte solution. The  $E_m$  observed is very similar to those found for copper hexacyanoferrate immobilized on different substrate surfaces.<sup>2,5,36</sup>



**Figure 4.** Cyclic voltammograms for SZC30/CuHCF in KCl 1.0 mol L<sup>-1</sup>. Scan rate from 5 up to 100 mV s<sup>-1</sup>.

The redox reaction shown in Figure 4 can be written as follows:



The cathodic and anodic peak separation,  $\Delta E_m$ , varies with scan rate increasing the potential sweeping velocity from 5 mV s<sup>-1</sup> ( $\Delta E_m = 0.017$  V) until 100 mV s<sup>-1</sup> ( $\Delta E_m = 0.11$  V), indicating the thickness of the film deposited on the substrate has influence on the electron transfer kinetic and the diffusion of K<sup>+</sup> into the CuHCF layer in order to keep the electroneutrality.<sup>37</sup> The thickness,  $d$ , of the CuHCF film on the substrate surface was estimated by applying equation 3:<sup>7</sup>

$$d = \frac{C}{nFA} \times \frac{l^3 N_0}{4} \quad (3)$$

where  $C$  is the value of integrated charge under the CV curve,  $l$  is the length of unit cell (10 Å),  $F$  is the Faraday constant,  $A$  is the area of electrode,  $N_0$  is the Avogadro's number and  $n$  is the number of electrons involved in the redox process. Assuming 4 as the number of effective Fe atoms in the unit cell, a film having approximately  $d = 101$  nm was estimated. It must be remembered that the value obtained is a rough estimation since it is not possible

in the process used to produce a film of CuHCF with spatial distribution control.<sup>38</sup>

#### *Influence of the K<sup>+</sup> concentration*

The cyclic voltammograms obtained with different concentrations of KCl supporting electrolyte solution show a linear correlation of the plot  $E_m$  vs.  $\log [K^+]$  (linear correlation,  $r = 0.999$ ,  $n = 6$ ), with a slope of the straight line of 0.059 *per* decade of potassium concentration, which indicates a Nernstian process. Assuming that the electroactive species is  $\text{KCu}[\text{Fe}^{\text{II}}(\text{CN})_6]^-$  and considering the redox process:



and the equilibrium reaction:



it can be demonstrated that,

$$E_m = E_s^0 + \frac{RT}{nF} \ln [K^+] \quad (6)$$

where  $E_s^0 = E^0 - \frac{RT}{nF} \ln \beta$ , and  $\beta$  is the equilibrium constant of the reaction represented in equation 5.

#### *Electrochemical impedance spectroscopy*

In order to determine the conducting character of the material, *i.e.*, the capacitive and diffusional processes that occur on the surface of the material, EIS measurements were made. Figure 5 shows the Bode diagram in the frequency interval between 100 kHz and 10 mHz. The result obtained

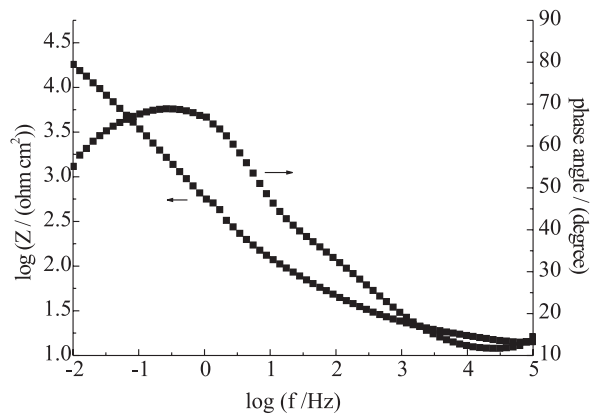


**Figure 5.** Bode diagram for SZC30 electrode in 1.0 mol L<sup>-1</sup> KCl solution. Applied potential: 0.69 V vs. SCE.

for the SZC30 electrode presents only one time constant at low frequency with a phase angle around 70 degrees, indicating a capacitive behavior influenced by the diffusion process of the electrolyte at the solid-solution interface.

Figure 6 shows the complex plane impedance plot for SZC30/CuHCF. The electron transfer resistance was determined from the intersection of the semicircle, which can be related to the charge transfer in oxidation-reduction, with the real axis at higher frequency in the Nyquist diagram. The values for electrolyte resistance,  $R_s = 7.2 \text{ ohm cm}^2$ , and polarization resistance,  $R_p = 31 \text{ ohm cm}^2$ , were determined. The value of charge transfer resistance,  $R_{ct}$ , where  $R_{ct} = R_p - R_s = 23.8 \text{ ohm cm}^2$ , is low and favors the oxidation-reduction reactions. This value is comparable, in magnitude, with CuHCF film chemically dispersed on C-films electrode surface, *i.e.*  $R_{ct} = 3 \text{ ohm cm}^2$ .<sup>32</sup>

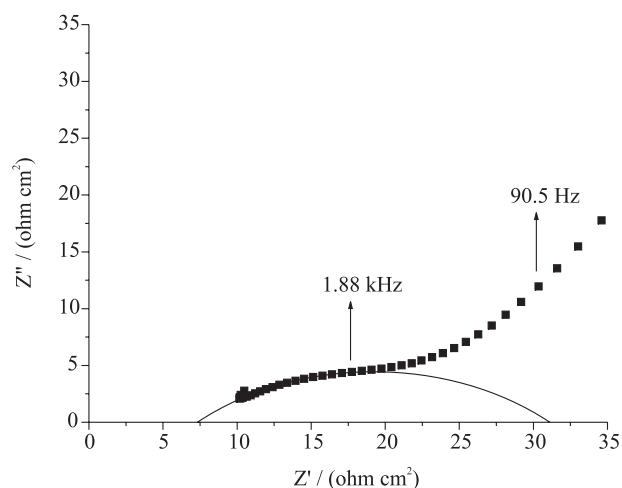


**Figure 6.** Nyquist diagram for SZC30/CuHCF electrode in  $1.0 \text{ mol L}^{-1}$  KCl solution in the high frequency range and simulated semicircle. Applied potential:  $0.69 \text{ V vs. SCE}$ .

Figure 7 shows the fit of a simulated and experimental Bode diagram for SZC30/CuHCF. The diagram can be interpreted using two time constants, the one at high frequency is due to the charge transfer process of the intervalence complex whereas the second, at low frequency, is attributed to the capacitive process including diffusion of  $K^+$  into the internal pores of the intervalence complex.<sup>37,39</sup>

The inset figure shows the equivalent circuit that best fits the experimental data for SZC30/CuHCF. The system is formed by two layers: 1) an external one that is formed by a capacitor  $C_1$  in parallel with resistance  $R_1$  of the layer and 2) a second internal layer that contains a capacitor  $C_2$  in parallel with the resistance of layer  $R_2$  and the Warburg impedance element ( $Z_w$ ) that measures the diffusion processes of the potassium ions at the electrode surface.

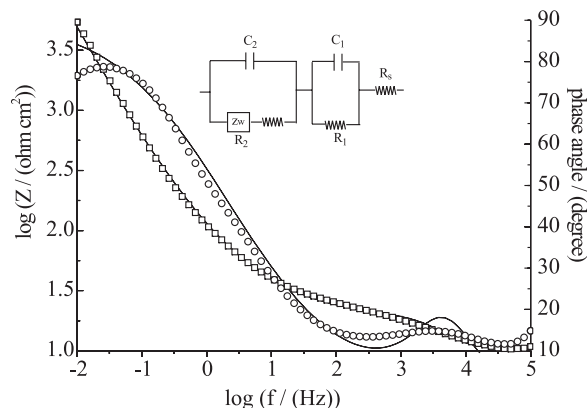


**Figure 7.** Experimental (square and open circles) and simulated (solid line) Bode diagram for SZC30/CuHCF electrode in  $1.0 \text{ mol L}^{-1}$  KCl solution. Applied potential:  $0.69 \text{ V vs. SCE}$ .

## Conclusions

The relatively high electric conductivity of the carbon ceramic materials, SZC20 and SZC30, are attributed to the high and homogeneous dispersion of C-graphite particles inside the matrices.

The immersion of SZC disks into the reagent solutions was described in the experimental part, resulted in a well structured copper hexacyanoferrate on the carbon ceramic electrode surface. The methodology of producing this film is very simple and reproducible and an advantage is that the surface can be renewed by polishing the disk surface and used again to produce the film.

The EIS results indicate that the oxidation/reduction reaction process in the SZC/CuHCF system occurs with a very low charge transfer resistance, *i.e.* the barrier of electron transfer through the copper hexacyanoferrate film is very low. Comparison of the EIS experimental data with the simulated results shows a charge transfer process at high frequency and a diffusion process into the pores at the solid/solution interface at lower frequencies.

## Acknowledgments

E.M., A.M.S.L. and M.S.P.F. are indebted to FAPESP for fellowships (Grants 04/00919-5, 02/12138-2 and 01/01248-9, respectively). Y.G. and R.L. are grateful to FAPESP (Grant 00/11103-5) for financial support. The authors thank R.C.G. Vinhas for technical assistance and Prof. C.H. Collins for manuscript revision.

## References

1. Tacconi, N. R.; Rajeshwar, K.; Lezna, R. O.; *Chem. Mater.* **2003**, *15*, 3046.

2. Mattos, I. L.; Gorton, L.; Laurel, T.; Malinauskas, A.; Karyakin, A. A.; *Talanta* **2000**, *52*, 791.
3. Narayanan, S. S.; Scholz, F.; *Electroanalysis* **1999**, *11*, 465.
4. Loos-Neskovic, C.; Ayrault, S.; Badillo, V.; Jimenez, B.; Garnier, E.; Fedoroff, M.; Jones, D. J.; Merinov, B.; *J. Solid State Chem.* **2004**, *177*, 1817.
5. Chen, Shen-Ming; Chan, Chia-Ming; *J. Electroanal. Chem.* **2003**, *543*, 161.
6. Cui, X.; Hong, L.; Lin, X.; *J. Electroanal. Chem.* **2002**, *526*, 115.
7. Siperko, L. M.; Kuwana, T.; *J. Electrochem. Soc.* **1983**, *130*, 396.
8. Zaldivar, G. A. P.; Gushikem, Y.; Kubota, L. T.; *J. Electroanal. Chem.* **1991**, *318*, 241.
9. Zaldivar, G. A. P.; Gushikem, Y.; *J. Electroanal. Chem.* **1992**, *337*, 165.
10. Kubota, L.; Gushikem, Y.; *J. Electroanal. Chem.* **1993**, *362*, 219.
11. Cunha, L. J. V.; Andreotti, E. I. S.; Gushikem, Y.; *J. Braz. Chem. Soc.* **1995**, *6*, 271.
12. Tsionsky, M.; Gun, G.; Glezer, V.; Lev, O.; *Anal. Chem.* **1994**, *66*, 1747.
13. Lev, O.; Wu, Z.; Bharati, S.; Glezer, V.; Modestov, A.; Gun, J.; Rabinovich, L.; Sampath, S.; *Chem. Mater.* **1997**, *9*, 2354.
14. Rabinovich, L.; Gun, J.; Lev, O.; Aurbach, D.; Markosvky, B.; Levi, M. C.; *Adv. Mater.* **1998**, *10*, 577.
15. Rabinovich, L.; Lev, O.; *Electroanalysis* **2001**, *13*, 265.
16. Salimi, A.; Poubeyram, S.; *Talanta* **2003**, *60*, 205.
17. Shul, G.; Sackek-Maj, M.; Opallo, M.; *Electroanalysis* **2004**, *16*, 1254.
18. Salimi, A.; Abdi, K.; *Talanta* **2004**, *63*, 475.
19. Salimi, A.; Abdi, K.; Khayatian, G.; *Electrochim. Acta* **2004**, *49*, 413.
20. Rozniecka, E.; Shul, G.; Sirieix-Plenet, J.; Guillon, L.; Opallo, M.; *Electrochem. Commun.* **2005**, *7*, 299.
21. Shul, G.; Opallo, M.; Marken, F.; *Electrochim. Acta* **2005**, *50*, 2315.
22. Salimi, A.; Nasiri, S.; Hadad, H.; Mohebi, S.; *Electroanalysis* **2005**, *17*, 2273.
23. Zaitseva, G.; Gushikem, Y.; *J. Braz. Chem. Soc.* **2002**, *13*, 611.
24. Alfaya, A. A. S.; Gushikem, Y.; Castro, S. C.; *Chem. Mater.* **1998**, *10*, 909.
25. Kurihara, L. A.; Fujiwara, S. T.; Alfaya, R. V. S.; Gushikem, Y.; Alfaya, A. A. S.; Castro, S. C.; *J. Colloid Interface Sci.* **2004**, *274*, 579.
26. Marafon, E.; Francisco, M. S. P.; Lucho, A. M. S.; Landers, R.; Gushikem, Y.; *Br PI 0506395-7*, **2005**.
27. <http://www.astm.org>, number F43-99, accessed in June 2005.
28. Parks, G.A.; *Chem. Rev.* **1965**, *65*, 177.
29. Ryczkowki, J.; *Catal. Today* **2001**, *68*, 263.
30. Scofield, J. H.; *J. Electron Spectrosc.* **1976**, *89*, 129.
31. JCPDS – International Centre for Diffraction Data. PCPDFWIN version 1.30, 1997.
32. Pauliukaite, R.; Florescu, M.; Brett, C. M. A.; *J. Solid State Electrochem.* **2005**, *9*, 354.
33. Cardoso, W. S.; Francisco, M. S. P.; Lucho, A. M. S.; Gushikem, Y.; *Solid State Ionics* **2004**, *167*, 165.
34. Moulder, J. F.; Stickle, W. F.; Sobol, P. E.; Bomben, K. D.; *Handbook of X-ray Photoelectron Spectroscopy*, Perkin-Elmer Corporation/Physical Electronics Division: Eden Prairie, 1992.
35. Barr, T. L.; *J. Phys. Chem.* **1978**, *82*, 1801.
36. Makowski, O.; Stroka, J.; Kulesza, P. J.; Malik, M. A.; Galus, Z.; *J. Electroanal. Chem.* **2002**, *532*, 157.
37. Kahlert, H.; Retter, U.; Lohse, H.; Siegler, K.; Scholz, F.; *J. Phys. Chem. B* **1998**, *102*, 8757.
38. Bharathi, S.; Nogami, M.; Ikeda, S.; *Langmuir* **2001**, *17*, 7468.
39. Juttner, K.; *Electrochim. Acta* **1990**, *35*, 1501.

Received: May 15, 2006

Published on the web: December 1, 2006

FAPESP helped in meeting the publication costs of this article.